UNIVERSITY OF NIŠ
The scientific journal **FACTA UNIVERSITATIS**
Series: **Mechanics, Automatic Control and Robotics** Vol.2, No 7/2, 1997 pp. 561 - 574
Editor of series: Katica (Stevanovi}) Hedrih, e-mail: katica@masfak.masfak.ni.ac.yu
Address: Univerzitetski trg 2, 18000 Niš, YU, Tel: (018) 547-095, Fax: (018)-547-950
http:// ni.ac.yu/Facta

THE UNSTABLE OPERATION OF TURBOMACHINES

UDC: 621.513; 621.43.031; 621.5.041; 621.51

Dragica Milenković

University of Niš, Faculty of Mechanical Engineering
Beogradska 14, 18000 Niš, Yugoslavia

Abstract. *The paper presents the results of the experimental and theoretical investigation of the rotating stall in the centrifugal compressor impeller assembled with the vaned and vaneless diffuser. The study of the phenomenon of the rotating stall in the centrifugal compressor stage has been accomplished by means of automated measuring complex. The objective of the obtained data analyses was determination of the rotating stall appearance. It has been found that two different kinds of stall exist, which points out to two different possibilities of the rotating stall origination.*

1. INTRODUCTION

It is well known that one or more areas of the opposite flow (which rotate in the direction of the rotor rotation) appear in the annular channel of the compressor during the gradual flow regulation through the compressor. This phenomenon is called the rotating stall and the regions of the opposite flow are called the stalled regions.

In many cases the transient to the rotating stall can lead to some undesirable consequences. An evident decrease of the pressure and of the flow is possible beyond the compressor, as well as the rapid decrease of the efficiency. The life time of the compressor blades is shortened which is caused by the tensions during the compressor operation in the region of the rotating stall. In regard to the above mentioned special attention has been paid to the rotating stall.

The analyses show that two different types of the stall are present during the decrease of the flow rate in the compressor and they differ in the rapid changes of the disturbance intensity, in the propagation speed and in the number of the stalled regions. The rotating stall consists of several small stalled regions in the areas of relatively high flow rates, and one or two big stalled regions appear in the areas of the low flow rates. In the first case the intensity of the disturbance is not so significant, but in the second one it is greater due to the opposite flow through the regions. These two forms of the rotating stall are called

Received September 16, 1997

the weak stall and the intensive stall.

The experiments show that during the rotating stall the phenomenon of the hysteresis is present, too; a slight difference can be noticed between the point of the rotating stall in the case of the flow decrease and the point of its disappearance in the flow increase. At the transition point there is a difference between the weak and the intensive stall, as well as the difference in the number of the stalled regions during the flow rate increase and decrease.

It is evident that the characteristics of the rotating stall depend on the concrete construction of the compressor [2]. Especially there is a great difference in the number of the stalled regions in the weak rotating stalls. In some compressors the weak stall does not exist at all - the intensive stall is present at the very beginning in such cases.

Considering the dimensions of the regions covered with the stall patches, two forms of the rotating stall can be mentioned: the partial stall - when the smaller stall patches cover only a part of the blade and the full stall - when the stalled region is extended to the full blade.

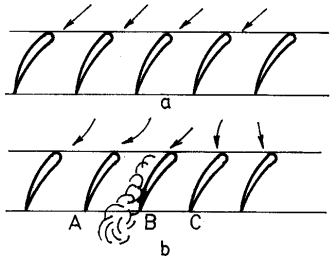

Fig. 1. The stalled regions during the flow over the profile lattice

The phenomenon of the rotating stall has been recognized in 1938. by a group of scientists [7] who had been working on the Whittle motor centrifugal compressors. Although the phenomenon had been recognized first in a centrifugal compressor, much more attention has been paid to the axial compressors in the later theoretical and experimental studies. However, all the theories were based on the small disturbances method. Although this method enables the prediction of the rotating stall beginning, it is quite useless in attempt to describe the uneven flow in the completely developed rotating stall. In the recent years nonlinear mathematical experiments [9] have been published. However, they are restricted to the discussion of the isolated rotor or a stage, and only 'qualitative ideas' are allowed to be obtained about some characteristics of the stalled regions. In regard to that, it is considered that the medium flow through the annular channel of the compressor remains constant during the process of transition from the flow without stall to the flow with rotating stall. In practice the operation point of the compressor depends on the installed valve and during the transient from the flow without stall to the completely propagated stall, the reduction of the pressure beyond the compressor can lead to a considerable change of the flow rate.

Although the number of the experimental studies is considerable, the studies mainly investigate the number of the stalled regions and the propagation speed. However, regardless to the detailed experimental material, nobody has succeeded in making a clear idea about the physical parameters which determine the basic flow characteristics with a

stall in an axial compressor up to now.

A simple drawing which can be used to explain the mechanism of the rotating stall is given in the figure 1 [6]. The lattice of an axial compressor which works at great angles of clearance is considered (fig. 1a). If any disturbances cause the local increase of the blade B angle of clearance (fig. 1b), the intensive rotating stall C of this blade will occur. Since the blade gap is narrowed due to the stalled region, the flow is separated from the blade B, which leads to an increase of the angle of clearance on the blade A and a decrease of the angle of clearance on the blade C.

The stall is extended from the right to the left, and in appropriate conditions it can be developed into fully propagated region extending along the lattice with the velocity V_p (Fig. 2).

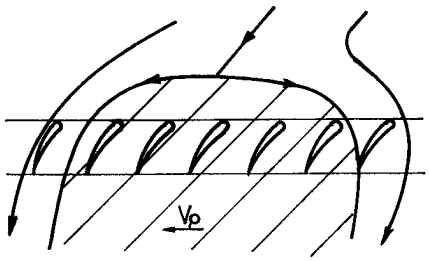

Fig. 2. Fully propagated stalled region

Such pattern of rotating stall development is accepted for the centrifugal compressors, too. The difference between axial and centrifugal machines is taken into consideration, and it is also emphasized that the investigation of the rotating stall in centrifugal machines is much more complex both from the experimental and theoretical point of view.

For the last ten years many intensive studies concerning non-stationary processes in the centrifugal compressor stage have been performed at the LPI M. I. Kalnina University, Leningrad [1,4,5].

The frequency of the rotating stall process is not known in advance. Besides, in the rotating stall the stalled regions are moving (‘rotating’) with angular velocity which is, as a rule, different from the frequency of rotation. In connection with this, the frequency of the process in the absolute coordinate system (the stationary elements of the flow sector) is different from the one in the relative coordinate system (the impeller).

As can be seen from the detailed investigations of the non-stationary processes in the centrifugal compressor, the measurement of the non-stationary pressures provides for the required idea about the character of the flow in the flow sector, especially when the measuring is done simultaneously on the rotating and stationary elements of the flow sector. According to the shape of the signal, pressure pulses can be divided into following types: constant, slow changing, periodical and random. The periodical oscillation parameters can be easily determined using the procedure of the synchronous accumulation when the beginning phase of the process and the period T are known. The algorithm of the synchronous accumulation has been accomplished by the developed informative-mathematical complex. The complex consists of: an analog measurement subsystem, synchronization and control subsystem, multi-channel statistic analyzers and

a mini computer, static and dynamic calibration subsystem and commutation elements.

An analog measuring subsystem consists of miniature pressure transducers (frequency of oscillations 70kHz, sensitivity 0.3÷0.9m/kPa on 3V), multi-point electricity governors, differential amplifiers and the amplitude-impulse modulators.

The experimental studies have been accomplished in the laboratory for the compressors of the LPI University, Leningrad. The subject of the present study has been the centrifugal compressor stage [10].

The impeller with $\beta_{L2} = 52^0$, diffuser with vanes ($\overline{D}_3 = D_3 / D_2 = 1.2$) and vaneless diffuser (Fig. 3 and Fig. 4) have been chosen for the investigation.

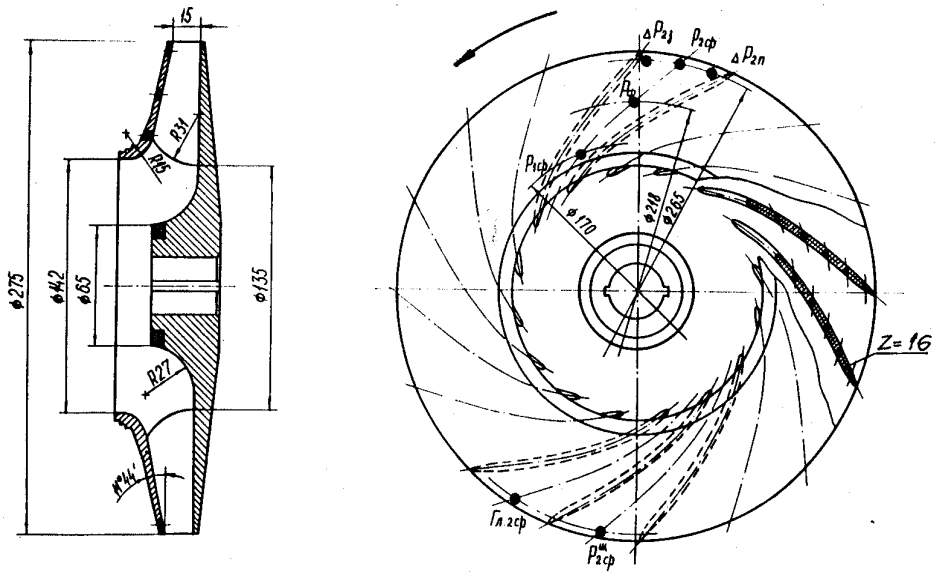

Fig. 3. The arrangement of the transducers in the impeller designed using the LPI method

The study of the rotating stall phenomenon in the centrifugal compressor stage has been accomplished by means of automated measuring complex mentioned above.

During the non-stationary pressure measurement the highest attention has been paid to the peripheral part of the impeller. The arrangement of the pressure transducers in the impeller and in the vaned diffuser is shown in the Fig. 3 and Fig. 4.

In all the cases the receivers of the pressure transducers were arranged so that they could measure the pulsation of the static pressure.

The parameters which indicate the appearance of the rotating stall were determined by means of the calculation according to the simultaneous indication of the transducers in the impeller, in the vane diffuser and vaneless diffuser. In addition, the number of the stalled regions Z_3 and the relative propagation speed $\overline{\omega}_3$ have been determined as for the axial compressor.

During the aerodynamic measurements performed in order to obtain the integral characteristics of the investigated compressor stage, the averaged total and static pressure, the temperatures and the angles of the stream flows were measured.

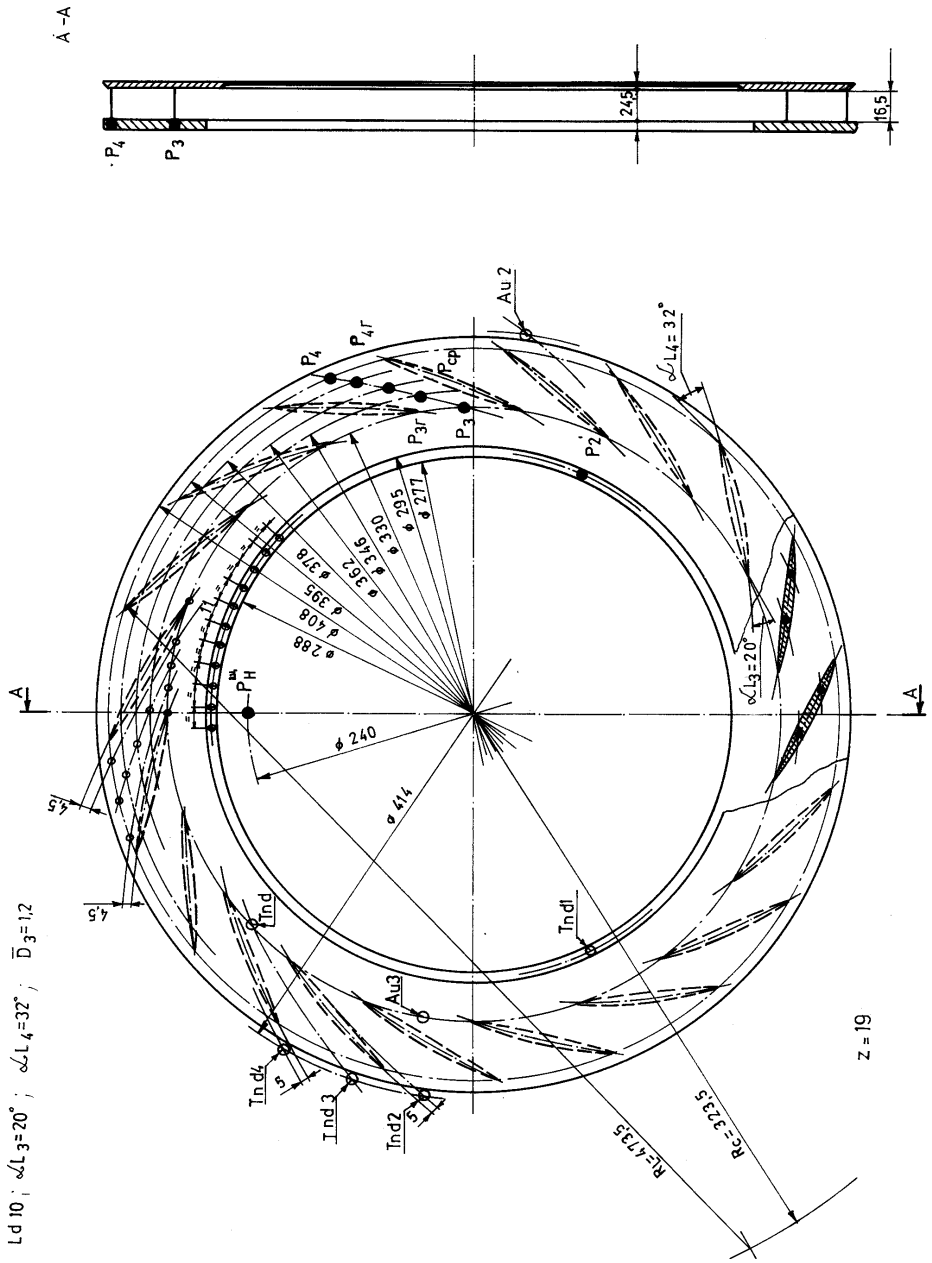

Fig. 4. The arrangement of the transducers in the vaned and vaneless diffusers

2. THE ANALYSES OF THE VISCOUS GAS FLOW IN A RADIAL VANELESS DIFFUSER

A great number of experimental studies [4] on the centrifugal compressors have been made in order to determine the main initiator of the rotating stall in the centrifugal compressor stage, but without any significant success. All the attempts have been directed to the determination of some characteristic values on the basis of which it has been said that the main initiator was the impeller, vane diffuser or vaneless diffuser, without any theoretical studying.

It is well known that all the studies of the centrifugal machines are complex and they require special mathematical apparatus. Therefore, it is not possible to describe with mathematical models the phenomena in the flow sector of the compressor, no matter how strongly we wish it. The flow of a viscous gas in a radial vaneless diffuser, which is a part of a centrifugal compressor, has been analyzed in this paper. The appropriate analyses have been made in order to determine the initiator of the rotating stall.

The turbulent boundary layer in the vaneless diffuser has been observed and we can start from the system of the equations as follows:

$$\begin{gathered} C_r\frac{\partial C_r}{\partial r}+C_z\frac{\partial C_r}{\partial z}-\frac{C_u^2}{r}=-\frac{1}{\rho}\frac{\partial p}{\partial r}+\frac{\partial}{\partial z}\left(\nu\frac{\partial C_r}{\partial z}-\overline{C_r'C_z'}\right) \\ C_r\frac{\partial C_u}{\partial r}+C_z\frac{\partial C_u}{\partial z}+\frac{C_rC_u}{r}=\frac{\partial}{\partial z}\left(\nu\frac{\partial C_u}{\partial z}-\overline{C_u'C_z'}\right) \\ \frac{\partial(C_r\cdot r)}{\partial r}+\frac{\partial(C_z\cdot r)}{\partial z}=0. \end{gathered} \tag{1}$$

The expressions for the tangential stress are given in the following form:

$$\tau_r=\mu\frac{\partial C_r}{\partial z}-\rho\overline{C_r'C'z}\,;\quad \tau_\varepsilon=\mu\frac{\partial C_u}{\partial z}-\rho\overline{C_u'C'z}\,. \tag{2}$$

In order to transform the system of equations (1) the usual designations were introduced:

R_2 - vaneless diffuser inlet radius;
C_{r2} - radial velocity component;
C_{u2} - circumferential velocity component;
$\mathrm{tg}\alpha = C_{r2}/\,C_{u2}$ - inlet flow angle to the vaneless diffuser.

In order to reduce the system (1) to nondimensional form the following designations were introduced:

$$\begin{gathered} \frac{C_r}{C_{r2}}\to\mathbf{C}_r\,;\quad \frac{C_u}{C_{u2}}\to\mathbf{C}_u\,;\quad \frac{C_z}{C_{uz}}\to\mathbf{C}_z\,; \\ \frac{p}{\rho C_{u2}}\to\mathbf{p}\,;\quad \frac{r}{R_2}\to\mathbf{r}\,;\quad \frac{z}{z_2}\to\mathbf{z} \end{gathered} \tag{3}$$

The pressure in the boundary layer in the considered case depends only on the radial component, so the pressure gradient is given with the following expression:

$$\frac{dp}{dr}=\frac{1}{r^3}(1+\alpha^2)\,. \tag{4}$$

Left sides of the first and the second equation of the system (1) were transformed and appropriate integration was done taking into account the boundary conditions:

$$z=0\,;\mathbf{C}_r=C_u=C_z=0\,;\ \tau_r=\tau_{rw}\,;\ \tau_\varepsilon=\tau_{\varepsilon w}\,;\ C_r=\mathbf{C}_r\,;\ C_u=\mathbf{C}_u\,;\ C_z=0\,;\ \tau_r=\tau_z=0\,. \quad (5)$$

After suitable grouping of the terms, the system (1) becomes the system of common differential equations:

$$\begin{aligned} &-\frac{\alpha}{r}\frac{d}{dr}\left[\frac{1}{r}\int_0^\infty(1-r^2\mathbf{C}_r{}^2)dz\right]+\frac{1}{r^3}\int_0^\infty(1-r^2\mathbf{C}_r{}^2)dz=-\frac{\tau_{rw}}{\rho\mathbf{C}_{u2}{}^2}\\ &-\frac{\alpha}{r^2}\frac{d}{dr}\left[\int_0^\infty(1-r^2\mathbf{C}_r\mathbf{C}_u)dz\right]=-\frac{\tau_{\varepsilon w}}{\rho\mathbf{C}_{u2}{}^2}. \end{aligned} \quad (6)$$

For the further work it is necessary to take into account the friction stresses τ_{rw} and $\tau_{\varepsilon w}$ at diffuser walls, and introduce the designations usual in the boundary layer theory:

$$\begin{aligned} &\delta_r^*=\int_0^\infty\left(1-\frac{C_r}{\mathbf{C}_r}\right)dz; \qquad \delta_r^{**}=\int_0^\infty\frac{C_r}{\mathbf{C}_r}\left(1-\frac{C_r}{\mathbf{C}_r}\right)dz; \qquad H_r=\frac{\delta_r^*}{\delta_r^{**}};\\ &\delta_\varepsilon^*=\int_0^\infty\left(1-\frac{C_r}{\mathbf{C}_r}\right)dz; \qquad \delta_\varepsilon^{**}=\int_0^\infty\frac{C_u}{\mathbf{C}_u}\left(1-\frac{C_u}{\mathbf{C}_u}\right)dz; \qquad H_\varepsilon=\frac{\delta_\varepsilon^*}{\delta_\varepsilon^{**}}. \end{aligned} \quad (7)$$

On the basis of experimental data for the velocity profile in the vaneless diffuser it was found that the tangential stresses were:

$$\begin{aligned} \tau_{rw}&=\frac{1}{2}\rho\mathbf{C}_r{}^2\cdot0.37\cdot10^{-0.85H_r}\cdot\mathrm{Re}_{\delta_r^{**}}^{-0.24}\\ \tau_{\varepsilon w}&=\frac{1}{2}\rho\mathbf{C}_u{}^2\cdot0.37\cdot10^{-0.85H_\varepsilon}\cdot\mathrm{Re}_{\delta_\varepsilon^{**}}^{-0.24}, \end{aligned} \quad (8)$$

where:

$$\mathrm{Re}_{\delta_r^{**}}=\frac{R_2C_r\mathbf{C}_{r2}\delta_r^{**}}{\nu}; \qquad \mathrm{Re}_{\delta_\varepsilon^{**}}=\frac{R_2C_u\mathbf{C}_{u2}\delta_\varepsilon^{**}}{\nu}. \quad (9)$$

In the case of turbulent boundary layer on the plain surface:

$$\tau_{\varepsilon w}=\frac{1}{2}\rho\mathbf{C}_u{}^2\cdot0.0238\cdot\mathrm{Re}_{\delta_\varepsilon^{**}}^{-0.24}. \quad (10)$$

Introducing new variables $u=r\mathbf{C}_\gamma$ and $v=r\mathbf{C}_u$, the following equations can be written:

$$\begin{aligned} &\delta_u^*=\int_0^\infty(1-u); \quad \delta_u^{**}=\int_0^\infty u(1-u)dz; \quad H_u=\frac{\delta_u^*}{\delta_u^{**}};\\ &\delta_v^*=\int_0^\infty(1-v); \quad \delta_v^{**}=\int_0^\infty v(1-v)dz; \quad H_v=\frac{\delta_v^*}{\delta_v^{**}}; \end{aligned} \qquad \delta_{uv}^{**}=\int_0^\infty(1-uv)dz\,. \quad (11)$$

Using the usual methods it can be shown that:

$$\begin{aligned} H_r &= H_u; \quad & \mathrm{Re}_{\delta_r^{**}} &= \frac{R_2 \mathbf{C}_{u2} \alpha \delta_u^{**}}{\nu r}; \\ H_\varepsilon &= H_v; \quad & \mathrm{Re}_{\delta_\varepsilon^{**}} &= \frac{R_2 \mathbf{C}_{u2}}{\nu} \frac{\delta_u^{**}}{r} \end{aligned} \tag{12}$$

Substituting the previous expressions into the system (6), it can be reduced to:

$$\begin{aligned} \frac{\alpha^2}{r} \frac{d}{dr}\left[\frac{(1+H_u)}{r}\delta_u^{**}\right] - \frac{2.4}{r^3}\delta_v^{**} &= 0.185 \cdot 10^{-0.85 H_u} \cdot \mathrm{Re}_{\delta_r^{**}}^{-0.24} \frac{\alpha^2}{r^2} \\ \frac{\alpha}{r^2}\frac{d\delta_{uv}^{**}}{dr} &= 0.0119\,\mathrm{Re}_{\delta_\varepsilon^{**}}^{-0.24} \frac{1}{r^2}. \end{aligned} \tag{13}$$

Boundary layer does not exist at the vaneless diffuser inlet, so the initial conditions are:

$$\delta_u^{**}\Big|_{r=1} = \delta_v^{**}\Big|_{r=1} = 0\,. \tag{14}$$

The equation system (13) is open, unless the connection among δ_{uv}^{**} and the requested values δ_u^{**}, δ_v^{**} and H_u were found. The procedure of recognizing those connections was given in the work [10].

The final form of the solved system is:

$$\begin{aligned} \frac{d}{dr}\left[\frac{(1+H)}{r}\delta_u^{**}\right] - \frac{2.4}{\alpha^2 r^2}\delta_v^{**} &= 0.815^{-0.85H}\,\mathrm{Re}_{\delta_r^{**}}^{-0.24}\frac{1}{r} \\ \frac{d\delta_{uv}^{**}}{dr} &= 0.0119\,\mathrm{Re}_{\delta_\varepsilon^{**}}^{-0.24}\frac{1}{\alpha} \\ \frac{d}{dr}(H_1\delta_u^{**}) &= F(H), \end{aligned} \tag{15}$$

where:

$$\begin{aligned} H_1 &= \frac{2H}{H-1}; \\ \mathrm{Re}_{\delta_r^{**}} &= \frac{\alpha\delta_u^{**}}{r}\frac{C_{u2}R_2}{\nu}; \\ \mathrm{Re}_{\delta_\varepsilon^{**}} &= \frac{C_{u2}R_2}{\nu}\frac{\delta_v^{**}}{r}; \\ \delta_{uv}^{**} &= H\delta_u^{**} + \frac{8.4\delta_v^{**}}{5}\left[\frac{(H-1)}{H(H+1)}\frac{8.4\delta_v^{**}}{\delta_u^{**}}\right]^{0.5(H-1)} \frac{2}{(H+1)\left[1.2+0.5(H-1)\right]}. \end{aligned} \tag{16}$$

The initial conditions are:

$$\delta_u^{**}\Big|_{r=1} = \delta_v^{**}\Big|_{r=1} = 0\,; \quad H\Big|_{r=1} = 1.5$$

The system of the equations was solved using Euler's method with the automatic choosing of the integration rate for small inlet angles to the vaneless diffuser ($\alpha_2 = 10^0 \div 20^0$) and for $\mathbf{C}_{u2} = 100 \div 200$m/s. On this basis a conclusion can be made that this values correspond to the experimental values. From numerous diagrams only one has been chosen as an illustration (Fig. 5) where the stalled limit in a vaneless diffuser was given for different values of the angle α_2 and for three values of $\mathbf{C}_{u2}$.

Practically the 'stalling' in the given case occurs when $\alpha_2 < 18^0$. These data agree quite well with the results of the experimental determination of the rotating stall limit in the stage with the vaneless diffuser. The obtained results about the stalling of the boundary layer on the walls of the vaneless diffuser and their parameters with the small angles α_2 were established on the idealized image of the flow in the vaneless diffuser, however they provide the possibility to grasp the physics of the flow process with a stall. It is considered that stalling represents the precursors of the rotating stall in the centrifugal compressor stage with vaneless diffuser.

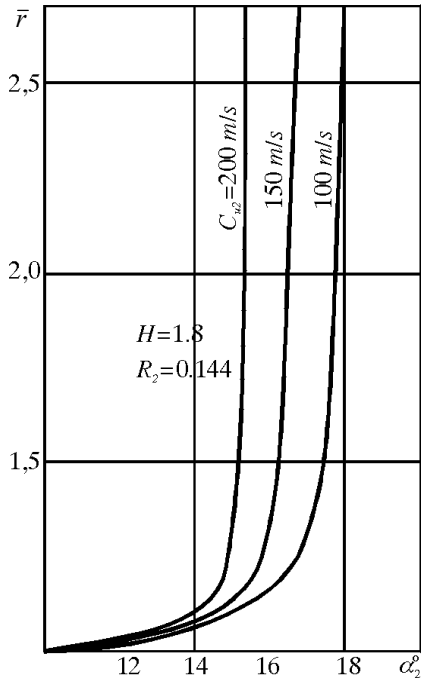

Fig. 5. The stalled limit in the vaneless diffuser

3. THE EXPERIMENTAL RESULTS

Figures 6, 7, 8, 9, 10 and 11 show the experimental diagrams of the compressor operating regimes for the velocities $U_2 = 100$, 150 and 196.4m/s and the Table 1 shows determined parameters of the rotating stall.

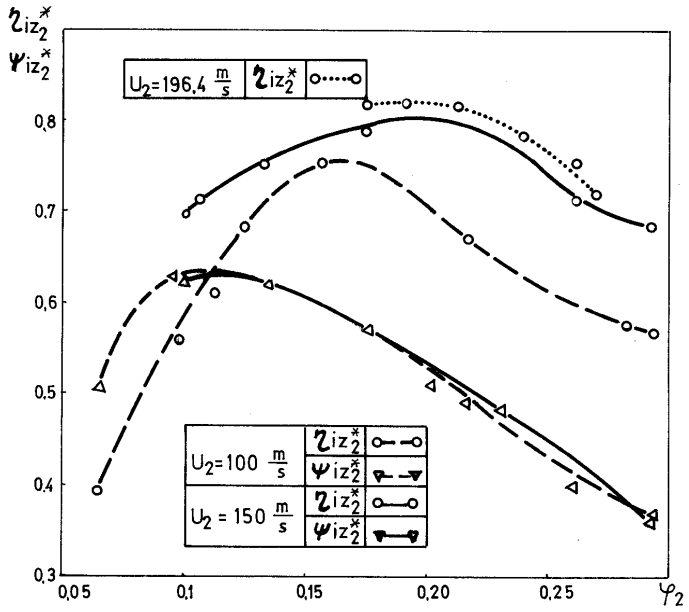

Fig. 6. Aerodynamic characteristics of the D43 stage

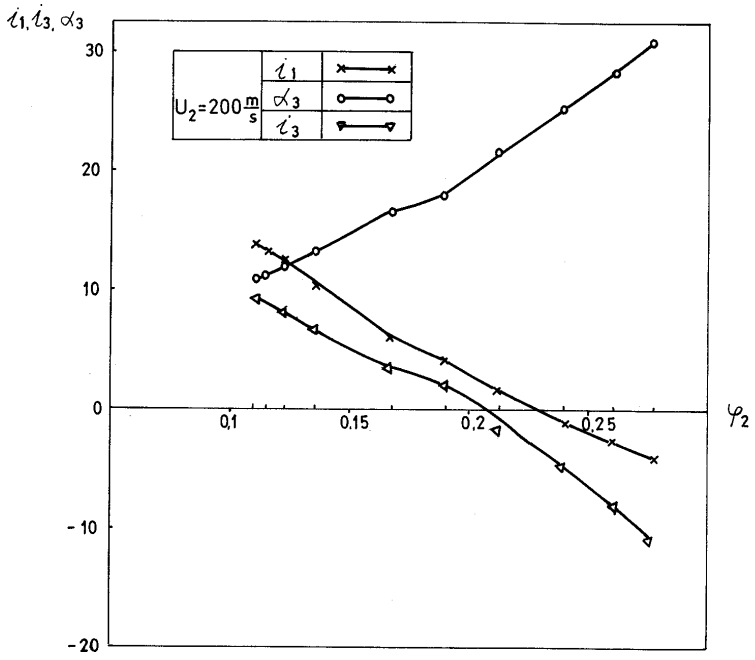

Fig. 7. The calculated angles i_1 , i_2 and i_3 as a function of φ_2

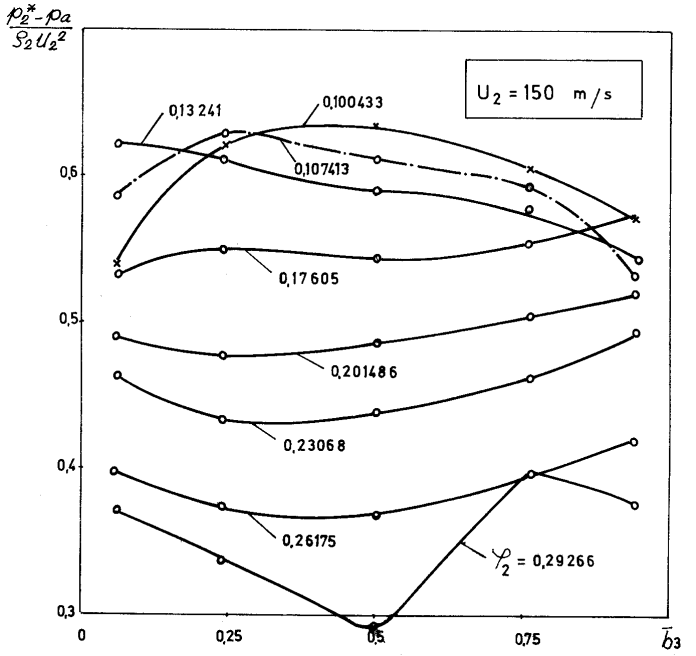

Fig. 8. The total pressure p_2^* arrangement along the width as a function of φ_2

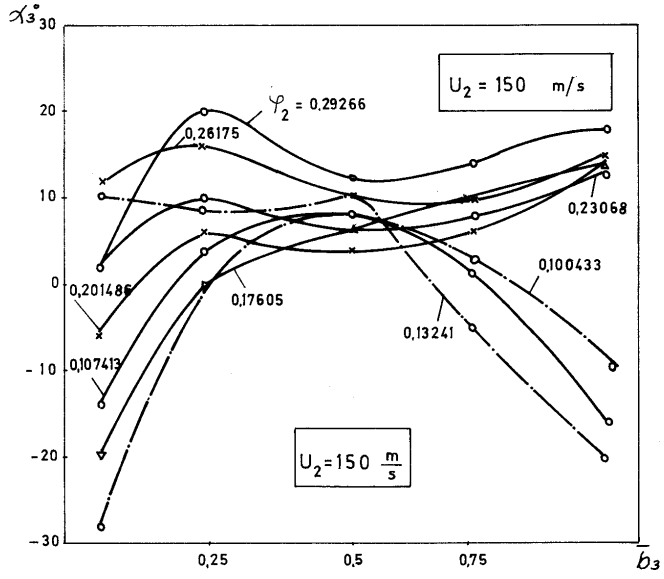

Fig. 9. The arrangement of the measured flow angles along the width as a function of φ_2

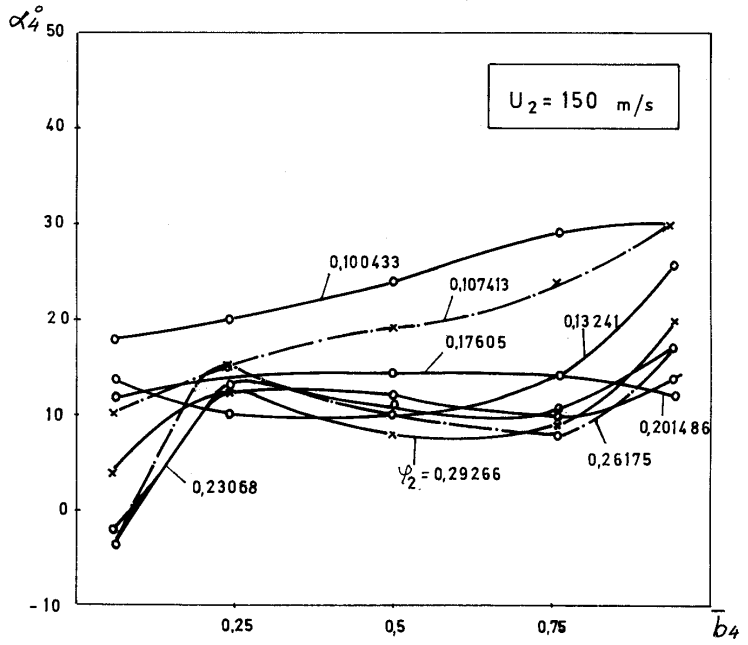

Fig 10. The arrangement of the measured flow angles along the width as a function of φ_2

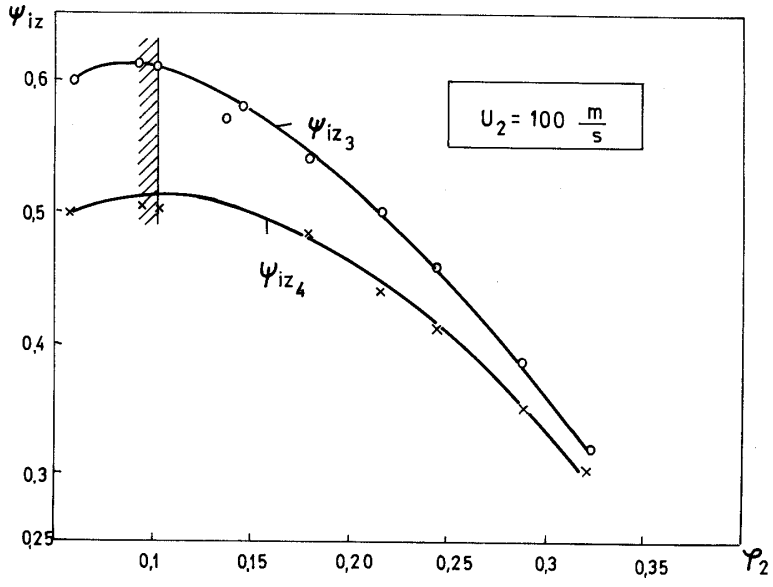

Fig 11. Aerodynamic characteristics of the D43 stage

TABLE 1. Main parameters which characterize the D45 stage operation during the unstable regimes

		Calculated values		Parameters of the stall		
	φ_0	i_1	α_3	z_3	$\bar{\omega}_3$	Notes
U_2=100m/s	0.1417	10.46	13.83	2	0.075	The limit of the stall
U_2=100m/s	0.1330	11.54	13.11	2	0.077	The stall
U_2=100m/s	0.1061	13.70	8.98	2	0.078	Chaotic oscillations
U_2=100m/s	0.0958	16.33	8.62	2	0.080	Stall with triple amplitude
U_2=100m/s	0.0766	18.89	7.49	2	0.083	Chaotic oscillations
U_2=100m/s	0.0600	21.12	5.60	2	0.091	The stall
U_2=150m/s	Regime 6			2	0.090	The stall
U_2=150m/s	Regime 7			2	0.083	Chaotic oscillations
U_2=150m/s	Regime 8			2	0.086	Developed stall
U_2=200m/s	Regime 3			2	0.082	The limit of the stall
U_2=200m/s	Regime 4			2	0.081	Weak stall
U_2=200m/s	Regime 5			2	0.080	Developed stall

Generalizing given results the following conclusions can be drawn:

1. With an increase of the circumferential velocity, the transitions move in the regions of higher flows.
2. The parameters of the rotating stall significantly depend on the circumferential velocity U_2 which can be seen from the enclosed table.
3. Different values of the angles α_3 and α_4 along the diffuser width correspond to the appearance limit of the rotating stall.
4. The arrangement of the total pressure over the cross section 2-2 along the diffuser width depends on the operating regime of the stage. The character of the pressure arrangement beyond the impeller is more uniform along the diffuser width at optimal operating regime.
5. The single-region stall differs from the multi-region stall by the character of forming.

REFERENCES

1. Akulêã in Ò. D., (1980) Izmaïlov i dr. *Ispolêzovanie IVK dlà issledovanià nestacionarnìh sluåaïnìh processov v turbomaã inah*, Meævuzovskï sbornik, Leningrad.
2. Borisov A., Lokãtanov E. A., Olêãteïn (1962) *Vraxaòxiïsàsrïv v osevom kompressore*, Primìãlenaà aèrodinamika nomer 24, Moskva.
3. Erãov V. N. (1966) *Neustoïåivìe reæimì turbomaã in*, Moskva.
4. Izmaïlov R. A. (1970) *Issledovanie nestacionarnìh processov v protoånoï åasti centrobeænogo kompressora*, Dis. na soiskanie uåenoï stepeni kand. tehn. nauk, Leningrad.
5. Izmaïlov R. A. (1980) *Razrabotka i primenenie informacionnogo - vìåisli-telênogo kompleksa dlà issledovanià nestacionarnìh teåeniï v centribeænìh kompressorah trudì* LPI nomer 370, Leningrad.
6. Stening A. (1980) *Vraxaòxiïsàsrìv i pompaæ*, Teoretiåeskie osnovì nomer 1.
7. Shesire L. J. (1945) *The Design and Development of Centrifugal Compressors for Aircraft Gas Turbines*, Institution of Mechanical Engineers Proceedings, Vol. 153 (War Emergency Issue No12)

8. Takata H. (1961) *Rotating stall in Multistage Axial Compressors*, Report of Aeronautical Research Institute, Universuty of Tokio, Vol. 2, No 6.
9. Takata Nagano (1972) *Nelineïnìï analiz vraxaòxegosà srìva, ènergetiåeskie maãinì i ustanovki*, nomer 4, izd-vo Mir.
10. Milenkovic Dragica (1988) *The Unstable Flows Through Impellers of the Turbomachines with the Stall*, doctorate, Belgrade.

NESTABILAN RAD TURBOMAŠINA

Dragica Milenković

U predloženom radu dati su rezultati eksperimentalnog i teorijskog ispitivanja karakteristika odvajanja (otkidanja) radnog kola centrifugalnog kompresora u sklopu s lopatičnim i bezlopatičnim difuzorom. Ispitivanje pojave otkidanja vrtloga u međustupnju centrifugalnog kompresora ostvareno je pomoću automatizovanog mernog kompleksa. Dobijeni podaci su analizirani u cilju određivanja inicijatora nastajanja pojave otkidanja vrtloga. Otkriveno je da postoje dve različite vrste otkidanja vrtloga, što govori o mogu}nosti dva mehanizma nastajanja otkidanja vrtloga.